Computing anode heating voltage in high-pressure arc discharges and modelling rod electrodes in dc and ac regimes

Computing anode heating voltage in high-pressure arc discharges and modelling rod electrodes in dc and ac regimes

N. A. Almeida, M. D. Cunha, and M. S. Benilov
Departamento de Física, FCEE, Universidade da Madeira,
Largo do Município, 9000 Funchal, Portugal
Instituto de Plasmas and Fusão Nuclear, IST,
Universidade de Lisboa, Portugal

Abstract

Numerical modelling of near-anode layers in arc discharges in several gases (Ar, Xe, and Hg) is performed in a wide range of current densities, anode surface temperatures, and plasma pressures. It is shown that the density of energy flux to the anode is only weakly affected by the anode surface temperature and varies linearly with the current density. This allows one to interpret the results in terms of anode heating voltage (volt equivalent of the heat flux to the anode). The computed data may be useful in different ways. An example considered in this work concerns the evaluation of thermal regime of anodes in the shape of a thin rod operating in the diffuse mode. Invoking the model of nonlinear surface heating for cathodes, one obtains a simple and free of empirical parameters model of thin rod electrodes applicable to dc and ac high-pressure arcs provided that no anode spots are present. The model is applied to a variety of experiments reported in the literature and a good agreement with the experimental data found.

Keywords: high-pressure arcs, near-electrode phenomena, arc-electrode interaction

1 Introduction

The interest in the modelling of plasma-electrode interaction in high-pressure arc discharges has significantly increased in the last couple of years [1–12]. Models of various levels of complexity have been developed for the plasma-cathode interaction. A comparison [2] has shown that in many situations one can use the so-called model of nonlinear surface heating, which is simple, may be readily applied to electrodes of complex shapes, and is ready for use for a wide range of plasma-producing gases and cathode materials. Plasma-anode interaction has been studied by means of complex numerical modelling; e.g., [4, 5, 13–16]. On the other hand, it is desirable to have also a simplified model of plasma-anode interaction, which could facilitate the development of fast and robust simulation tools for applications.

In this connection, one of the objectives of this work is to theoretically validate the concept of volt equivalent of the heat flux to the anode, which is also called anode heating voltage. This quantity is derived from a modelling of near-anode layers in arc discharges in several gases in a wide range of current densities, anode surface temperatures, and plasma pressures.

The computed values of the anode heating voltage may be used in various ways. As an example, in this work these values are employed in order to complete the approximate model of thin rod anodes proposed in [17, 18] and to obtain, with the use of the model of nonlinear surface heating for cathodes, a simple and free of empirical parameters model of rod electrodes applicable to dc and ac high-pressure arcs in cases where no anode spots are present. The model is applied to conditions of various experiments reported in the literature and a good agreement found. The latter may be considered as an experimental validation of both the approach and the computed values of the anode heating voltage. This allows one to employ these values for analysis of interaction of high-pressure plasmas with anodes in other situations, e.g., for simulation of interaction of an LTE arc plasma with a planar water-cooled anode as was done in [19].

The outline of the paper is as follows. In section 2, results of calculation of the energy flux to anodes are reported for plasmas of high-pressure arc discharges in Ar, Xe, and Hg arc in a wide range of current densities, anode surface temperatures, and plasma pressures, and are interpreted in terms of anode heating voltage. Application to rod electrodes of high-pressure arcs is considered in section 3. Conclusions are summarized in section 4.

2 Volt equivalent of the heat flux to the anodes of high-pressure arc discharges

The concept of volt equivalent of the heat flux to electrode is a popular tool for approximate analysis of plasma-electrode interaction in high-pressure arc discharges; e.g., [20] and references therein and [21] as a more recent example. This concept is based on the assumption that the power input Q from the plasma to the electrode is proportional to the arc current I:

$$Q = IU_h, \tag{1}$$

where the proportionality coefficient U_h (the electrode heating voltage, or volt equivalent of the heat flux to the electrode) may depend on the plasma-producing gas and its pressure and on the electrode material. Assuming that U_h is known, one can estimate the integral power input from the plasma to the electrode for any given arc current.

A straightforward way to theoretically validate the concept of electrode heating voltage is to analyze results of the unified numerical modelling, where the whole near-electrode layer is described by the single set of equations, including the Poisson equation, without apriori dividing the layer into quasi-neutral plasma and space-charge sheath. Such modelling has been performed in two dimensions in space in the recent work [22] for a low-current gliding arc. For strongly ionized plasmas of high-current arcs, such modelling has been performed in one dimension in space up to now [4, 12, 13, 23], which is justified by the near-electrode layer being thin. An example of results of such modelling for the case of cathode is depicted by the solid line in figure 1. The modelling in this example includes solving the equations describing the near-cathode layer jointly with the thermal-conduction equation in the cathode body as described in section 3 of [2]. The lateral surface of the cathode is assumed to be electrically and thermally insulated in these simulations, therefore the temperature distribution inside the cathode varies only in the axial direction and all parameters are constant along the cathode surface. The assumption (1) in this example is equivalent to

$$q = jU_h, \tag{2}$$

where q and j are the densities of energy flux and electric current from the plasma to the electrode. However, figure 1 clearly shows that there is no proportionality between q and j in any meaningful sense. Hence, the concept of volt equivalent of the heat flux to the electrode is not applicable to the case of cathode.

Results of the unified numerical modelling of near-anode layers of atmospheric-pressure arc discharges are shown in figure 2 for three plasma-producing gases (Ar, Xe, and Hg). In contrast to the modelling shown in figure 1, the one shown in figure 2 did not include solving the thermal-conduction equation inside the electrode body, therefore the anode surface temperature T_w needed to be specified as an input parameter and was varied in a wide range. One can see that the approximation (2) is quite reasonable in the case of anodes. The energy flux density and, therefore, the value of U_h are virtually independent of the anode temperature.

Beyond the 1D case, the temperature of the anode surface differs substantially from one point of arc attachment to the other (in contrast to the case of the cathode). Furthermore, the anode temperature varies strongly with the arc current, again in contrast to the case of the cathode. Since, however, the computed anode heating is independent of the anode temperature as mentioned above, equation (2) gives rise to equation (1) and the concept of volt equivalent of the heat flux to the electrode is theoretically justified in the case of anode.

Values of the anode heating voltage U_h for Ar, Xe, and Hg under atmospheric pressure are close to each other and equal to approximately 6.1. Results of similar simulations for different plasma pressures p are summarized in table 1. (We note for accuracy that the values of U_h for $p = 10$ and 100 bar have been derived from simulations performed for $T_h = 1500, 2500, 3500$ K, since pressures above 1 bar are of interest primarily in connection with high-intensity discharge lamps, which usually operate with hot electrodes.) One can see that U_h is virtually independent of plasma pressure for Xe in the whole range $p = 1 - 100$ bar. The anode heating voltage for Ar is virtually independent of p in the range $p = 1 - 10$ bar and weakly increases with an increase in p in the range $p = 10 - 100$ bar. For Hg, U_h weakly increases with an increase in p in the range $p = 1 - 10$ bar; the increase of U_h with p in the range $p = 10 - 100$ bar is more appreciable, although still not very strong.

Note that the data given in table 1 have been derived from simulations performed in the range of current densities j up to 10^7 A m^{-2}, as seen in figure 2. This range is appropriate for most applications; for example, the computed maximum value of current density at the surface of a planar copper anode of a 200 A atmospheric-pressure Ar arc is about $(1.25 - 1.6) \times 10^6$ A m^{-2} depending on the model [6, 19]. On the other hand, the current density on anodes of very-high pressure high-intensity discharge lamps may reach values of several times 10^7 A m^{-2} [13]. In this connection, the energy flux densities in the current density range of up to 10^8 A m^{-2} are shown in figure 3 for Xe and Hg, which are the usual buffer gases in high-intensity discharge lamps, at $p = 100$ bar. One can see that the approximation (2) remains applicable with the values of U_h which are virtually independent of T_w and equal 5.7 V for Xe and 7.1 V for Hg. Note that the latter values are different from those obtained for the current density range $j \leq 10^7$ A m^{-2}, which are given in the last column of table 1.

A similar unified modelling of near-anode layers of very high-pressure xenon and mercury arcs, reported in [13] for the electrode temperature range $2000 - 3500$ K, the plasma pressure range $50 - 200$ bar, and the current densities of 10^7 and 10^8 A m^{-2}, gave U_h in the range $5.6 - 5.8$ V for xenon and and $6.7 - 9.4$ V for mercury. (Note that the anode heating voltage was determined in [13] for each value of j as the value of the ratio q/j, rather than by fitting the dependence $q(j)$ in a wide range of j as in this work. Therefore, the values of U_h of this work are not exactly the same as the corresponding values reported in [13].) A model of ablating

graphite anode of a 79 kPa helium arc, developed in [5], has shown that the anode heating voltage is virtually independent of the ablation rate, provided that this rate is not high, and is about 6 V.

The assumption (1) for the case of anode is supported also by experimental data. In particular, the experiments [24], performed with tungsten rod electrodes of different dimensions in a 2.6 bar Ar arc, are well described by the relation (1) with $U_h = 6.24\,\mathrm{V}$ [25]. The latter value is close to 6.1 V, which is the value obtained by the linear interpolation over p of the corresponding data in table 1. A similar linear behavior was found for a tungsten anode operating in a xenon plasma under the pressure of about 100 bar [13], with U_h about 5.4 V. Again, this is close to the corresponding computed value given in table 1 (5.9 V).

Thus, the concept of electrode heating in the case of anodes conforms to both experiment and the modelling.

Note that current transfer across the near-anode layer of a high-pressure arc is a complex phenomenon involving a number of different mechanisms. Contributions of different mechanisms to the energy flux to the anode have been analyzed in [13]; cf. equations (8) and (10) of [13]. The biggest single contribution is given by condensation of electrons at the anode surface. The linear approximation (2), while being reasonable, is nevertheless only an approximation, as is clearly seen from figure 2b and is attested by the above-mentioned difference in the values of U_h obtained in the different current density ranges for Xe and Hg at $p = 100\,\mathrm{bar}$. Note also that the concept of anode heating voltage may become inapplicable in cases where current transfer to the anode is affected by a cathode jet; e.g., [26].

The modelling allows one to compute the anode heating voltage U_h in a self-consistent way for a wide range of conditions without invoking empirical data. In particular, the computed values of the anode heating voltage for Ar, Xe, and Hg may be taken from table 1 and figure 3. The only parameter of the anode material used in the simulations is the work function, which was set equal to 4.5 eV (work function of tungsten and copper; the metals most frequently used). If there is a need to re-scale the heating voltage to an anode material with a different (say, lower) work function, the natural first guess will be to subtract the difference of the work functions from the value of U_h computed in this work.

3 Modelling rod electrodes of dc and ac arc discharges

Knowing the anode heating voltage, one can evaluate the power input from the plasma to the anode for a given arc current. In the particular case of anodes having the shape of a thin rod, which are used in high-intensity discharge lamps, and a diffuse current transfer, this information is sufficient to approximately determine the thermal regime of the anode. The procedure is as follows. The distribution of temperature T inside the body of an electrode, anode or cathode, and at its surface is governed by the thermal-conduction equation,

$$\rho c_p \frac{\partial T}{\partial t} = \nabla \cdot (\kappa \nabla T)\,. \tag{3}$$

Here t is time, ρ, c_p and κ are, respectively, mass density, specific heat, and thermal conductivity of the electrode material. The Joule heating inside the electrode body is not essential in most cases and is not taken into account.

The boundary condition for equation (3) at the base of the electrode is governed by the particular experimental arrangement and should be specified case-by-case. The boundary con-

dition at the top and lateral surfaces of the electrode is written as

$$\kappa \frac{\partial T}{\partial n} = q, \tag{4}$$

where n is the external normal to the electrode surface and q is the density of net energy flux from the plasma to the electrode (which describes all the mechanisms of energy exchange between the plasma and the electrode, including cooling of the electrode by radiation and, in the case of cathode, by electron emission).

If the electrode operates as an anode (anode of a dc arc or an electrode of an ac arc during the anodic phase), one can evaluate, by means of equation (1), the total power input from the plasma to the anode, i.e., the integral of function q over the anode surface for a given I. In the general case, this information is not sufficient to determine thermal regime of the anode: one needs to know the power distribution over the anode surface (i.e., function q). However, an exception exists: if the anode has the shape of a thin rod and operates in the diffuse mode, then its thermal regime is not appreciably affected by the way in which the current is distributed over the anode top. For example, one can assume, following [17], that the arc current and the power input are localized at the front surface of the anode and distributed in a uniform way over this surface. In other words, one can find thermal regime of the anode by solving equation (3) with the boundary condition (4), assuming that the function q is constant at the front surface of the anode and vanishes at the lateral surface.

In this way, one obtains a closed thermal model of thin rod anodes of high-pressure arcs, operating in the diffuse mode. The model does not contain empirical parameters and is simple and easy to implement.

In order to compute ac regimes, the above anode model should be combined with a simple model for cathodes. The concept of volt equivalent of the heat flux to the electrode is not applicable to the case of cathode. However, one can resort to the model of nonlinear surface heating, which is computationally simple enough. (For example, the model of nonlinear surface heating is implemented in the Internet tool [27] for rod cathodes of dc arcs, which simulates in an automated way the diffuse mode of current transfer and modes with axially symmetric spots for a wide range of plasma-producing gases and cathode materials.) This model does not rely on arbitrary assumptions, is self-consistent, and has been validated by extensive comparison with the experiment and more complex models; e.g., [2, 28, 29]. An example of such comparison is seen in figure 1, where results of simulations by means of the model of nonlinear surface heating are depicted by the dotted line. One can see that the dependence $q(j)$ computed by means of the model of nonlinear surface heating is in a good agreement with the one given by the unified modelling; a conclusion which applies also to other integral characteristics of the plasma-cathode interaction [2].

It is of interest to compare the above-described model for the anodes and the model of nonlinear surface heating from the methodological point of view. The model of nonlinear surface heating exploits the fact that a significant electric power is deposited by the arc power supply into the near-cathode layer. Power deposited into the near-anode layer is not significant and may be even negative, which is why the model of nonlinear surface heating is not applicable to anodes. In the framework of the model of nonlinear surface heating, the rhs of the boundary condition (4) is evaluated as a function not of the position on the electrode surface, as in the case of anodes, but rather of the value of the local temperature T_w. More precisely, q and j the density of electric current from the plasma to the cathode surface are computed by means of a suitable model of near-cathode layer as functions of T_w and the near-cathode voltage drop

U: $q = q(T_w, U)$, $j = j(T_w, U)$. It should be stressed that, although distributions of densities of the energy flux and electric current over the cathode surface remain unknown at this stage, knowing the function $q = q(T_w, U)$ is sufficient for solving the equation (3) with the boundary condition (4) for U given. After this equation has been solved, one will be able to evaluate the distributions of densities of the energy flux and electric current over the cathode surface in terms of the functions $q(T_w, U)$ and $j(T_w, U)$ and the computed distribution of the cathode surface temperature T_w. This is in contrast to the model for the anodes, where the current and energy flux distribution over the electrode surface is assumed rather than computed.

Let us proceed to comparison with the available experimental data on rod electrodes operating in anode and ac regimes. Results for the cathode regime are also included for completeness. The modelling has been performed for tungsten electrodes of argon, mercury, and xenon arcs. Data on thermal conductivity and emissivity of tungsten have been taken from [30] and [31], respectively; parameters of the near-cathode plasma layer have been computed by means of the model summarized in [32].

Figure 4 shows the dependence of the anode tip temperature on the arc current in a dc arc in the 2.6 bar-argon plasma under conditions of the experiment [24]. The temperature at the base of the electrode was set equal to 300 K and calculations have been performed with $U_h = 6.1$ V, which is the value obtained by the linear interpolation over p of the corresponding data in table 1. Solid lines in figure 4 depict the simulations performed with the arc current uniformly distributed over the front surface of the anode. Dashed lines refer to the modelling with the arc current being uniformly distributed over the front surface and an adjacent part of the lateral surface of height equal to the electrode radius. The solid and dashed lines are quite close; a proof that thermal regime of thin rod anodes is not appreciably affected by the way in which the current is distributed over the anode top.

Also shown in figure 4 are experimental data [24]. The agreement between the calculation results and experimental data is reasonably good. Note that the accuracy of the model should be approximately the same for all the electrodes that the figure refers to, which is proved by the proximity of the solid and dashed lines. Hence, a better agreement seen in figure 4 for electrodes of smaller diameters can hardly be attributed to a higher accuracy of the model for such electrodes; it may be just a coincidence or maybe even an indication of a somewhat higher error of the experiment for wider electrodes.

Figure 5 shows the computed tip temperature of a rod electrode of a dc 2.6 bar-argon arc under conditions of the experiments [24, 33], operating in the anode and cathode regimes. Also shown are experimental data. The agreement between the modelling and the experiment is good.

Results of simulations of electrodes of a 2.6 bar-argon arc powered by switched dc (square-wave) current under conditions of the experiment [34] are shown in figure 6. The temperature at the base of the electrode was set equal to 300 K and calculations of the anodic phase have been performed with $U_h = 6.1$ V as above. The anode voltage drop, which has to be specified in order to evaluate the electrode sheath voltage, was set equal to 4 V according to [24]. (We remind that the model computes the cathode voltage drop, but not the anode one.) Also shown are the experimental data. The agreement between the modelling and the experiment is good.

The above-mentioned value of 4 V for the anode fall was reported in [24] for dc arcs with anodes of radii of 0.3, 0.5, and 0.75 mm in the arc current range $2-4$ A. On the other hand, the measurements [34] have shown that the anode fall for ac arcs under comparable conditions varies only marginally during the half-cycle and is almost independent of the arc current; however the quantitative result was different: 2 V. If the latter value is used, the absolute values of the

computed electrode sheath voltage in figure 6 will be reduced by 2 V and the agreement with the experiment will be more or less the same.

Results of simulations of electrodes of a 17 bar-mercury arc powered by a switched dc current under conditions of the experiment [18] are shown in figure 7. There is not enough information on the electrode cooling arrangement in [18], so a fixed temperature of 1000 K was assumed at 10 mm from the electrode tip. Calculations of the anodic phase have been performed with $U_h = 7\,\mathrm{V}$, which is the value obtained by the linear interpolation over p of the corresponding data in table 1. The agreement between the modelling and the experiment is good.

Figure 8 shows the calculated power input from a 100 bar-xenon dc arc into the electrodes operating in the anode and cathode regimes under conditions of the experiment [13]. The geometry of the electrode in the modelling was the one shown in figure 4 of [13]; roughly speaking, the electrode was a rod of radius of 0.2 mm and height of 2 mm with a hemispherical tip. Thermal measurements reported in [13] indicated that the temperature and energy flux at the base of the electrode obey the relation $T = 300\pi R^2 \kappa\, \partial T/\partial z + 800$ (in SI units; the z-axis is directed along the electrode axis from the base to the tip, R is the radius of the base of the electrode). This relation was used as a boundary condition in the modelling. While simulating the anode regime, it was assumed that $U_h = 5.9\,\mathrm{V}$, which is the corresponding value from table 1, and that the current is collected by, and uniformly distributed over, the hemispherical tip.

Two axially symmetric solutions have been found in the calculations performed for the cathode regime. One of these solutions describes the diffuse mode and exists for all currents. The other solution describes the spot mode, exists for $I \lesssim 0.8\,\mathrm{A}$, and comprises two branches separated by a turning point: the high- and low-voltage branches, with the high-voltage branch being associated with a slightly higher voltage and a hotter spot. Note that the power input from the power supply into the near-cathode region is higher on the high-voltage branch, however, a part of this power transported by the electron current into the bulk is higher as well, so the power input into the cathode is lower as seen in figure 8b. The theory [35, 36] predicts that the low-voltage branch is unstable, the high-voltage branch is stable and therefore should occur in the experiment.

Also shown in figure 8 are experimental data [13]. When the electrode operated as anode, the current transfer occurred in the diffuse mode in the whole current range investigated in the experiment. When the electrode operated as cathode, current transfer occurred in the spot mode for low currents, $I \lesssim 0.8\,\mathrm{A}$, and the diffuse mode for higher currents, $I \gtrsim 0.9\,\mathrm{A}$.

The agreement between the modelling and the experiment is good in figure 8. In particular, the measurements are in agreement with the theoretical prediction that it is the high-voltage branch that occurs in the experiment. The switching from the spot mode to the diffuse mode on the cathode is accompanied by a noticeable increase in the power input; a feature well known from both experiment and modelling (e.g., [17, 28]).

4 Concluding remarks

Two simple approaches to simulation of electrodes of high-pressure arc discharges are described in the literature: the so-called model of nonlinear surface heating and the approximate model based on the concept of electrode heating voltage (volt equivalent of heat flux). The model of nonlinear surface heating exploits the fact that a significant electric power is deposited by the arc power supply into the near-cathode layer. Power deposited into the near-anode layer is not significant and may be even negative, therefore the model of nonlinear surface heating, while

being applicable to cathodes, does not apply to anodes. In contrast, the concept of electrode heating voltage is not applicable to cathodes (there is no proportionality between the energy flux from the arc to a cathode and the arc current in any meaningful sense), however represents a good approximation for anodes.

In this work, unified modelling of near-anode layers of high-pressure arc discharges is performed for three plasma-producing gases (Ar, Xe, and Hg) in a wide range of current densities, anode surface temperatures, and plasma pressures. It is shown that the density of energy flux to the anode is virtually independent of the anode surface temperature and varies linearly with the current density; a result that represents a theoretical justification of the concept of anode heating voltage. The computed values of the anode heating voltage are summarized in table 1.

The computed data may be useful in different ways. In particular, these data allow one to evaluate thermal regime of the anode in the shape of a thin rod operating in the diffuse mode. Invoking the model of nonlinear surface heating for cathodes, one obtains a simple and free of empirical parameters model of thin rod electrodes applicable to dc and ac high-pressure arcs in cases where no anode spots are present.

A model obtained in this way gives results in agreement with the available experimental data. This agreement may be considered as an experimental validation of both the model and the computed values of the anode heating voltage for conditions of thin rod electrodes of low-currents arcs, which are typical of high-intensity discharge lamps and to which the available experimental data, treated in this work, refer. On the other hand, the anode heating voltage does not depend on the shape of the anode being considered. Therefore, the computed values of the anode heating voltage may be used for analysis of arc plasma-anode interaction in other situations. In particular, in [19] these data are used for simulation of interaction of an atmospheric-pressure argon arc with the arc current 20 to 200 A, described in the LTE approximation, with a planar water-cooled copper anode.

Acknowledgments The work was supported by FCT - Fundação para a Ciência e a Tecnologia of Portugal through the project Pest-OE/UID/FIS/50010/2013.

References

[1] M. Alaya, C. Chazelas, G. Mariaux, and A. Vardelle, J. Thermal Spray Tech. **24**, 3 (2015).

[2] M. S. Benilov, N. A. Almeida, M. Baeva, M. D. Cunha, L. G. Benilova, and D. Uhrlandt, J. Phys. D: Appl. Phys. **49**, 215201 (2016).

[3] T. Chen, C. Wang, M.-R. Liao, and W.-D. Xia, J. Phys. D: Appl. Phys. **49s**, 085202 (2016).

[4] I. L. Semenov, I. V. Krivtsun, and U. Reisgen, J. Phys. D: Appl. Phys. **49**, 105204 (2016).

[5] V. A. Nemchinsky and Y. Raitses, Plasma Sources Sci. Technol. **25**, 035003 (2016).

[6] M. Baeva, M. S. Benilov, N. A. Almeida, and D. Uhrlandt, J. Phys. D: Appl. Phys. **49**, 245205 (2016).

[7] A. J. Shirvan, *Modelling of cathode-plasma interaction in short high-intensity electric arc. Application to Gas Tungsten Arc Welding*, Ph.D. thesis, Chalmers University of Technology, Gothenburg, Sweden (2016).

[8] A. J. Shirvan and I. Choquet, Welding in the World **60**, 821 (2016).

[9] M. Baeva, Plasma Chem. Plasma Process. **36**, 151 (2016).

[10] M. Baeva, Plasma Chem. Plasma Process. **37**, 341 (2017).

[11] T. Chen, C. Wang, X.-N. Zhang, H. Zhang, and W.-D. Xia, Plasma Sources Sci. Technol. **26**, 025002 (2017).

[12] A. Khrabry, A. Khodak, I. Kaganovich, V. Vekselman, and V. Nemchinsky, in *2017 IEEE Int. Conf. on Plasma Sci. (ICOPS)* (2017).

[13] N. A. Almeida, M. S. Benilov, U. Hechtfischer, and G. V. Naidis, J. Phys. D: Appl. Phys. **42**, 045210 (11pp) (2009).

[14] S. Tashiro, M. Tanaka, and A. B. Murphy, Surf. Coat. Tech. **205**, S115 (2010), proceedings of the 7th Asian-European Inernational Conference on Plasma Surface Engineering AEPSE 2009.

[15] J. P. Trelles, Plasma Sources Sci. Technol. **22**, 025017 (2013).

[16] J. P. Trelles, Plasma Sources Sci. Technol. **23**, 054002 (2014).

[17] G. M. J. F. Luijks, S. Nijdam, and H. v Esveld, J. Phys. D: Appl. Phys. **38**, 3163 (2005).

[18] G. M. J. F. Luijks, H. A. van Esveld, S. Nijdam, and P. A. M. Weerdesteijn, J. Phys. D: Appl. Phys. **41**, 144006 (5pp) (2008).

[19] M. Lisnyak, M. D. Cunha, J.-M. Bauchire, and M. S. Benilov, J. Phys. D: Appl. Phys. (2017), 10.1088/1361-6463/aa76d3.

[20] P. Teste, T. Leblanc, J. Rossignol, and R. Andlauer, Plasma Sources Sci. Technol. **17**, 035001 (2008).

[21] V. A. Nemchinsky and Y. Raitses, J. Phys. D: Appl. Phys. **48**, 245202 (2015).

[22] S. Kolev, S. Sun, G. Trenchev, W. Wang, H. Wang, and A. Bogaerts, Plasma Process. Polym. **14**, 1600110 (2017).

[23] N. A. Almeida, M. S. Benilov, and G. V. Naidis, J. Phys. D: Appl. Phys. **41**, 245201 (26pp) (2008).

[24] M. Redwitz, L. Dabringhausen, S. Lichtenberg, O. Langenscheidt, J. Heberlein, and J. Mentel, J. Phys. D: Appl. Phys. **39**, 2160 (2006).

[25] J. Mentel and J. Heberlein, J. Phys. D: Appl. Phys. **43**, 023002 (2010).

[26] J. Heberlein, J. Mentel, and E. Pfender, J. Phys. D: Appl. Phys. **43**, 023001 (2010).

[27] M. S. Benilov and M. D. Cunha, "On-line tool for simulation of different modes of axially symmetric current transfer to cathodes of high-pressure arc discharges, version 3," (2009, http://www.arc_cathode.uma.pt/tool).

[28] M. S. Benilov, J. Phys. D: Appl. Phys. **41**, 144001 (30pp) (2008).

[29] L. Dabringhausen, O. Langenscheidt, S. Lichtenberg, M. Redwitz, and J. Mentel, J. Phys. D: Appl. Phys. **38**, 3128 (2005).

[30] Y. S. Touloukian, R. W. Powell, C. Y. Ho, and P. G. Clemens, *Thermal Conductivity. Metallic Elements and Alloys*, Thermophysical Properties of Matter, vol. 1 (IFI/Plenum, New York-Washington, 1970).

[31] S. W. H. Yih and C. T. Wang, *Tungsten: Sources, Metallurgy, Properties, and Applications* (Plenum Press, New York, 1979).

[32] M. S. Benilov, M. D. Cunha, and G. V. Naidis, Plasma Sources Sci. Technol. **14**, 517 (2005).

[33] L. Dabringhausen, D. Nandelstädt, J. Luhmann, and J. Mentel, J. Phys. D: Appl. Phys. **35**, 1621 (2002).

[34] O. Langenscheidt, S. Lichtenberg, L. Dabringhausen, M. Redwitz, P. Awakowicz, and J. Mentel, J. Phys. D: Appl. Phys. **40**, 415 (2007).

[35] M. S. Benilov, J. Phys. D: Appl. Phys. **40**, 1376 (2007).

[36] M. S. Benilov and M. J. Faria, J. Phys. D: Appl. Phys. **40**, 5083 (2007).

gas \ p (bar)	1	10	100
Ar	6.1	5.9	6.7
Xe	6.1	5.8	5.9
Hg	6.1	6.8	9.5

Table 1. Computed anode heating voltage.

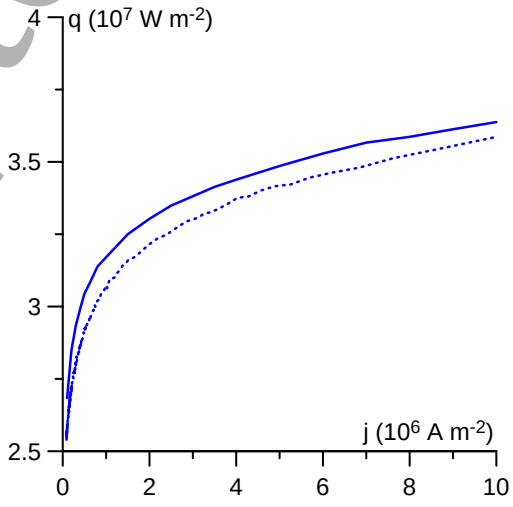

Figure 1. Density of energy flux from the plasma to the cathode of atmospheric-pressure arc discharge in argon. Cylindrical tungsten cathode with an insulating lateral surface, height of 10 mm, and the room temperature at the base. Solid: the unified modelling (the code [23]). Dotted: the model of nonlinear surface heating (the Internet tool [27]).

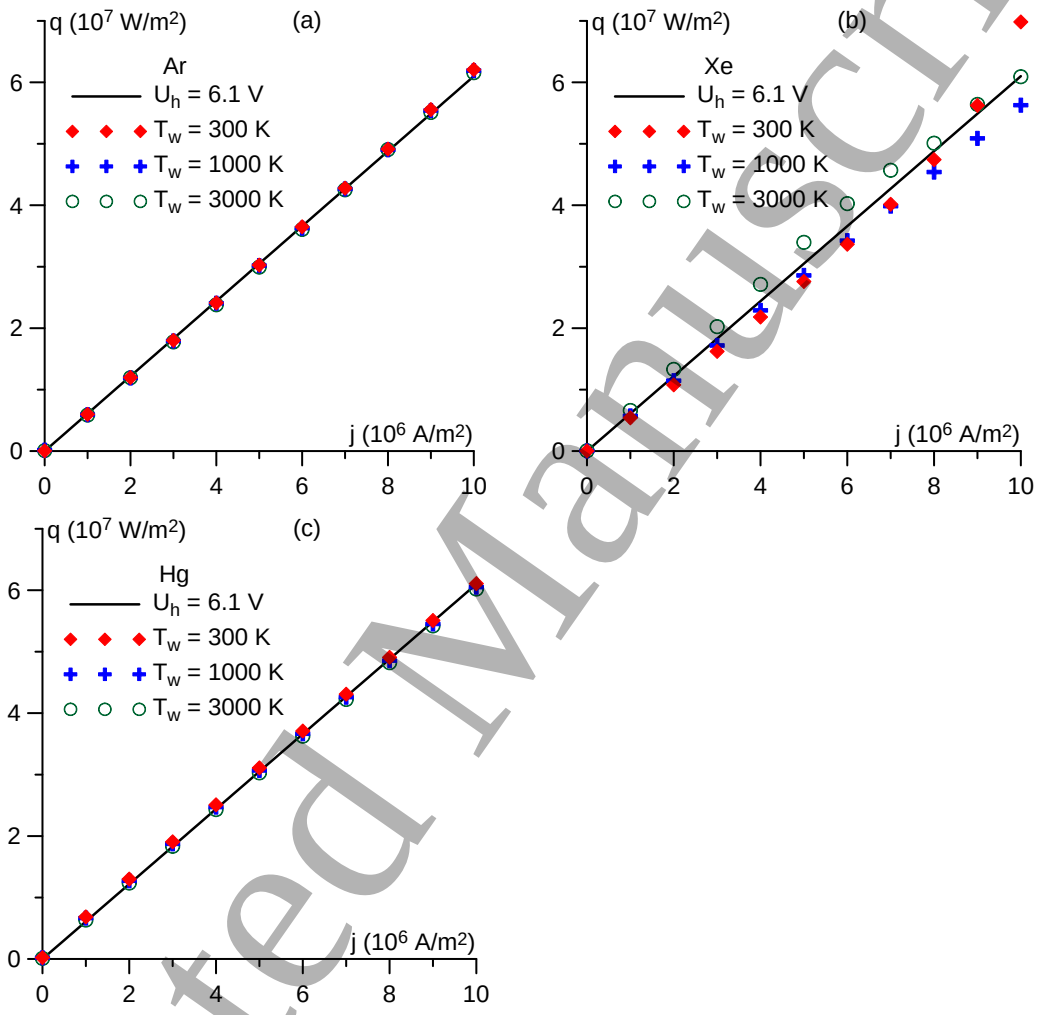

Figure 2. Density of energy flux from the plasma to the anode of arc discharges in atmospheric-pressure gases for different values of the anode surface temperature. Points: the unified modelling of near-anode layers (the code [13]). Line: dependence $q = jU_h$ with $U_h = 6.1$ V.

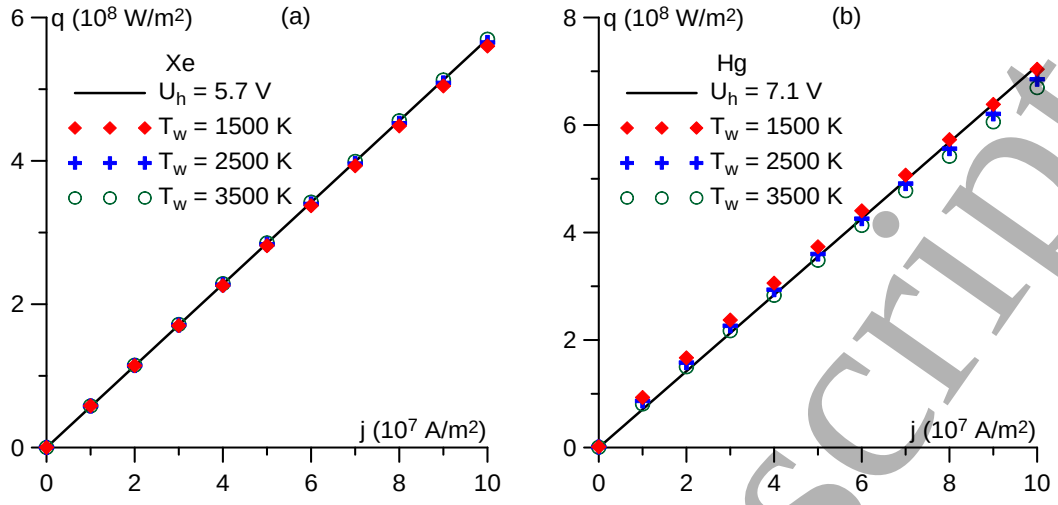

Figure 3. Density of energy flux from the plasma to the anode of arc discharge in 100 bar Xe and Hg in a wide range of current densities. Points: the unified modelling of near-anode layers (the code [13]). Line: dependence $q = jU_h$ with U_h equal to 5.7 V (a) and 7.1 V (b).

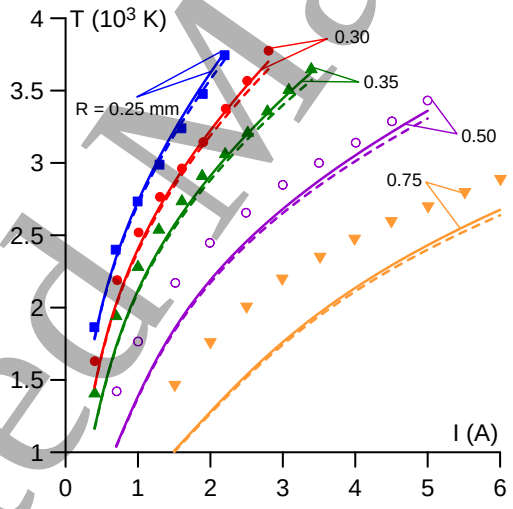

Figure 4. Tip temperature of rod tungsten anodes of height of 20 mm and variable radii R. Dc 2.6 bar-argon arc with a diffuse anode attachment. Solid, dashed: modelling. Points: experiment [24].

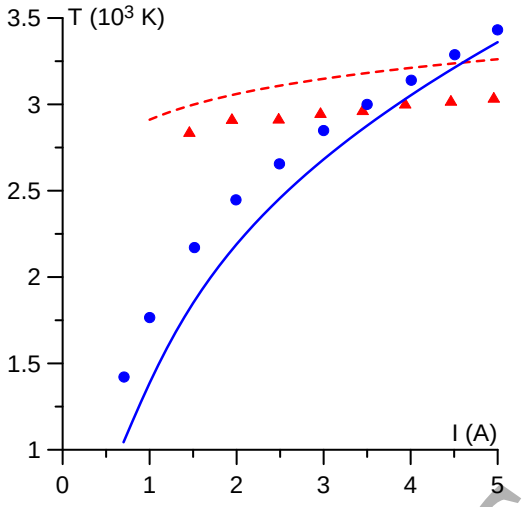

Figure 5. Tip temperature of a rod tungsten electrode of radius of 0.5 mm and height of 20 mm. Dc 2.6 bar-argon arc with diffuse electrode attachments. Solid: anode, modelling. Circles: anode, experiment [24]. Dashed: cathode, modelling. Triangles: cathode, experiment [33].

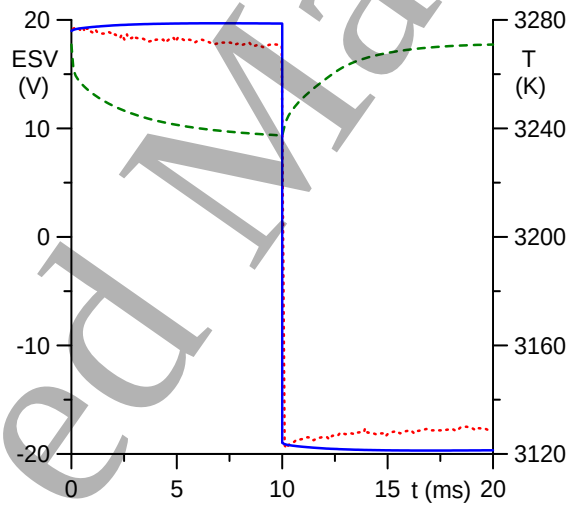

Figure 6. Solid: electrode sheath voltage, modelling. Dotted: electrode sheath voltage, experiment [34]. Dashed: tip temperature, modelling. Tungsten electrode of radius of 0.5 mm and height of 20 mm, 2.6 bar-argon arc, switched dc current of amplitude of 4.24 A and frequency of 50 Hz.

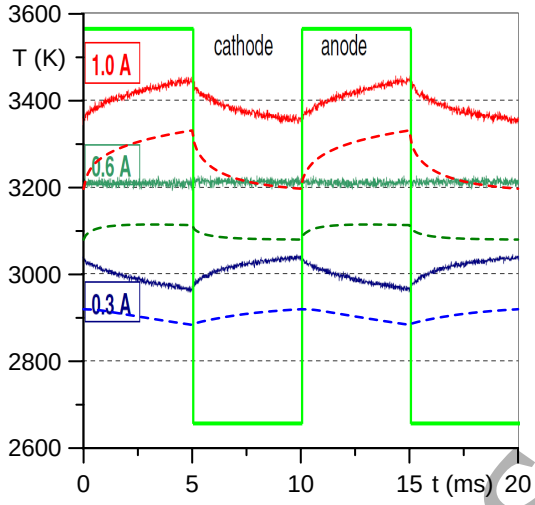

Figure 7. Tip temperature of a rod tungsten electrode of radius of 0.18 mm and height of 10 mm. 17 bar-mercury arc, switched dc current of different amplitudes and frequency of 100 Hz. Dashed: modelling. Solid: experiment [18].

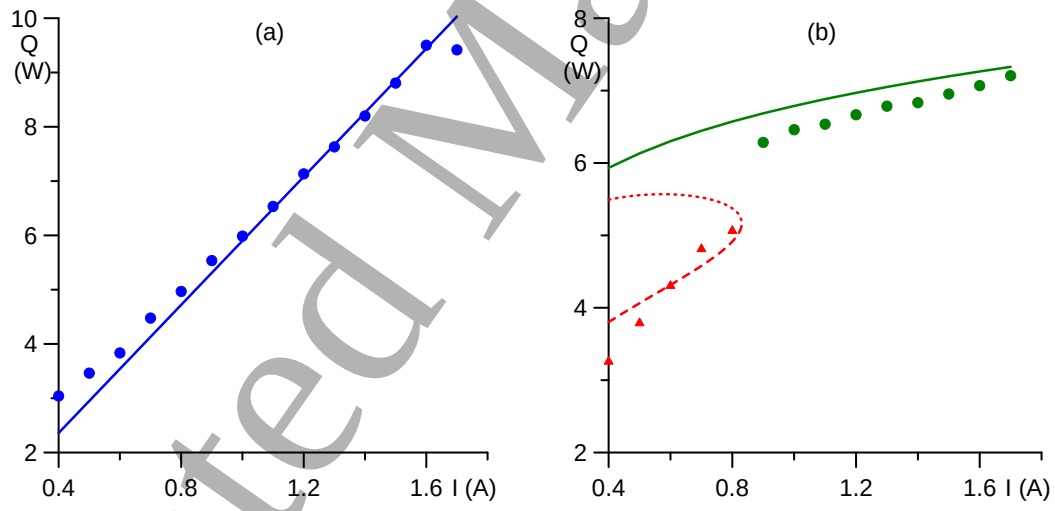

Figure 8. Power input to the rod anode (a) and cathode (b) of a dc 100 bar-xenon arc. Solid: diffuse mode, modelling. Circles: diffuse mode, experiment [13]. Dashed: modelling, the high-voltage branch of the spot mode. Dotted: modelling, the low-voltage branch of the spot mode. Triangles: spot mode, experiment [13].